Contract No:

This document was prepared in conjunction with work accomplished under Contract No. DE-AC09-08SR22470 with the U.S. Department of Energy.

Disclaimer:

AFM CHARACTERIZATION OF RAMAN LASER INDUCED DAMAGE ON CdZnTe CRYSTAL SURFACES

Lucile C. Teague*, Samantha A. Hawkins, and Martine C. Duff, *Savannah River National Laboratory, Aiken, SC 29808*

Arnold Burger, Michael Groza, and Vladimir Buliga, *Fisk University, Nashville, TN 37208-3051*

*To whom correspondence should be addressed.

E-mail: lucile.teague@srnl.doe.gov

Keywords: CZT, CdZnTe, atomic force microscopy, Raman, radiation detection

Introduction

High quality CdZnTe (or CZT) crystals have the potential for use in room temperature gamma-ray and X-ray spectrometers.[1, 2] Over the last decade, the methods for growing high quality CZT have improved the quality of the produced crystals however there are material features that can influence the performance of these materials as radiation detectors. The presence of structural heterogeneities within the crystals, such as twinning, pipes, grain boundaries (polycrystallinity), and secondary phases (SPs) [3-11] can have an impact on the detector performance. There is considerable need for reliable and reproducible characterization methods for the measurement of crystal quality. With improvements in material characterization and synthesis, these crystals may become suitable for widespread use in gamma radiation detection.

Characterization techniques currently utilized to test for quality and/or to predict performance of the crystal as a gamma-ray detector include infrared (IR) transmission imaging, synchrotron X-ray topography, photoluminescence spectroscopy, transmission electron microscopy (TEM), atomic force microscopy (AFM) and Raman spectroscopy.[1, 6, 7, 12-26] In some cases, damage caused by characterization methods can have deleterious effects on the crystal

performance. The availability of non-destructive analysis techniques is essential to validate a crystal's quality and its ability to be used for either qualitative or quantitative gamma-ray or X-ray detection. The work presented herein discusses the damage that occurs during characterization of the CZT surface by a laser during Raman spectroscopy, even at minimal laser powers.

Previous Raman studies have shown that the localized annealing from tightly focused, low powered lasers results in areas of higher Te concentration on the CZT surface.[16] This type of laser damage on the surface resulted in decreased detector performance which was most likely due to increased leakage current caused by areas of higher Te concentration. In this study, AFM was used to characterize the extent of damage to the CZT crystal surface following exposure to a Raman laser. AFM data reveal localized surface damage and increased conductivity in the areas exposed to the Raman laser beam.

Materials and Methods

Two different CZT crystals (CZT3-7-4 and 3-7-8) were used in this study and were obtained from Yinnel Tech (South Bend, IN). They were grown by the modified vertical Bridgman (MVB) method[27] and are composed of ~ 10% Zn content ($Cd_{1-x}Zn_xTe$, with x=0.1). Both faces of the crystal were finely polished with a series of alumina grit sizes; the finest of which was 0.05 μm.

CZT3-7-4 was identified as a moderate performer for gamma-ray spectrometry using an ^{241}Am source (Figure 1). Both the Cd-terminating face and the Te-terminating face of this crystal were exposed to an Argon ion laser (514.5 nm) in a Raman microscope system. Using the Raman laser, a series of highly damaged fiducial marks (~20 mW) were created as well as a

series of lower laser power exposure areas (~160 mW to 1.7 mW) for subsequent AFM evaluation (see Figure 2). Raman spectra were collected simultaneously with the surface laser exposure with a 100X objective and a cooled charge-coupled device (CCD) camera detector. The Raman spectra of the untreated, freshly polished surface are consistent with those reported previously,[16] and were collected with lower laser power (less than 100 μW) in order to reduce the damage to the crystal.

The surface of CZT3-7-8 was also exposed to a Raman laser (632.8 nm, HeNe) in four different regions for ~30 seconds (s) each. Previous studies of this crystal showed that while it has a high concentration of SPs within the crystal, the detector performance was not adversely influenced.[6]

The AFM topographic and conductive probe images were collected for the laser damaged regions on both crystals in contact mode in an ambient atmosphere. The aforementioned fiducial marks in the laser damaged region of CZT3-7-4 were easily located using the optical microscope of the AFM, and the AFM tip was positioned over the region of the laser damage for AFM analysis. For C-AFM measurements on CZT3-7-8, conductive Ti/Pt coated tips were used to image the area while a bias potential was applied to the CZT crystal.

Results and Discussion

The Raman spectra of the laser damaged regions between 160 μW and 1.7 mW on the Cd-terminating face are shown in Figure 3. At lower laser powers, Raman peaks are observed at ~125, 145, and 175 cm^{-1}. The peak at ~120 cm^{-1} corresponds to Te.[28] The peaks at ~145 and ~175 cm^{-1} have previously been assigned to the transverse optic (TO) and longitudinal optic (LO) modes of CdTe respectively.[21-26]

During prolonged exposure to the laser, even at very low power, the peak at ~125 cm^{-1} grows to the most intense peak of the spectrum, while no other new peaks appear. As previously shown, the peak at ~145 cm^{-1} also becomes more intense with higher power laser exposure whereas the peak at ~175 cm^{-1} does not. This behavior has been compared to that of melted Te metal.[16] This suggests that the laser, being focused very tightly on the surface, even at low power, causes a localized surface annealing effect and the enrichment of Te relative to the surrounding bulk CZT material. Thermomigration has been suggested as a probable mechanism to explain the increase in Te concentration near the heated area.[29] It is possible that free Te atoms migrate to the heated areas. However, AFM measurements suggest that Cd vaporization may also explain the increase in Te near laser treated areas (in the absence of a Cd vapor overpressure as in these studies).

AFM data of laser exposed regions reveal the amount of surface damage is related to the laser power and time elapsed during surface exposure, with some observable damage even at very low laser powers (~1 mW). Figure 4 shows an AFM image and line scan of one of the fiducial marks (created at high laser power) on the Cd-terminating face. In contrast, Figure 5 shows the topographic and lateral force (friction) AFM images for laser-treated areas on both faces of the CZT crystal. On the Cd-terminating face, the regions exposed to the laser at ~425 μW (200 s) and ~1.7 mW (80 s) are not visible in the topographic images; however, some contrast is observed in the friction image for the region exposed to the laser at ~1.7 mW for 80 s. On the Te-terminating face, the regions exposed to the laser at ~1.7 mW (both 40 s and 80 s) show contrast in the friction image, with some topographic changes also observed for both. Even when there is no observable damage in the topographic images, the observed contrast in the friction images reveals that there is a difference in the tip-sample interaction at the location of

Raman laser exposure. This finding suggests that the surface composition was sufficiently modified by the laser.

C-AFM was also used to investigate the surface of CZT3-7-8 surface following exposure to a Raman laser in four different regions. Each region was exposed to the laser for ~30s (11 mW) resulting in holes in the surface ~4 μm wide and ~800 nm deep. C-AFM images taken with a +7 V bias applied to the CZT crystal show regions of increased conductivity at the edges of the laser induced damage (Figure 6). Topographic images show that these areas of increased conductivity correspond to a pile-up of material that occurs on the edges of the laser damaged areas—consistent with a combination of both of the aforementioned hypotheses that (1) Cd material is being evaporated from the surface and (2) free Te atoms are migrating to these heated areas. These data, in combination with previous Raman results,[16] suggest that the increased conductivity is a result of a localized increase in Te in the areas exposed to the laser. We also note that the difference in conductivity between the Te rich laser damaged areas and the surrounding bulk is an order of magnitude smaller than that of similar C-AFM studies of surface-terminated Te rich SPs. This difference is most likely due to the nature of the surface Te metal present for each case. It is expected that the thickness of Te redeposited on the surface during laser exposure is <200 nm, in contrast to the amount of Te material in the surface terminated Te-rich SPs (~10 μm).

Conclusions

The CZT surface has been exposed to a Raman laser in a controlled fashion to elucidate the amount of damage caused during Raman analysis. AFM studies reveal that the degree of surface damage to the crystal is dependent on the laser power and exposure time, with the

greatest observable damage occurring at higher laser power and exposure times. These data are consistent with Raman spectra showing the largest increase in Te signal at higher laser power. These Raman and AFM studies suggest that localized annealing occurs in the regions directly exposed to the laser beam. C-AFM studies reveal that these highly damaged regions are also regions of increased conductivity, further supporting the observed increase in Te at these regions.

Acknowledgements

This work was supported by the U.S. Department of Energy (US DOE) - National Nuclear Security Administration, through the Office of Nonproliferation Research and Engineering (NA-22) and National Science Foundation through the Fisk University Center for Physics and Chemistry of Materials (CPCoM), Cooperative Agreement CA: HRD-0420516 (CREST program) and through and from US DOE NA-22, Grant No. DE-FG52-05NA27035. The authors would also like to thank Dr. Eliel Villa-Aleman for providing access to the Raman laser system.

Figures

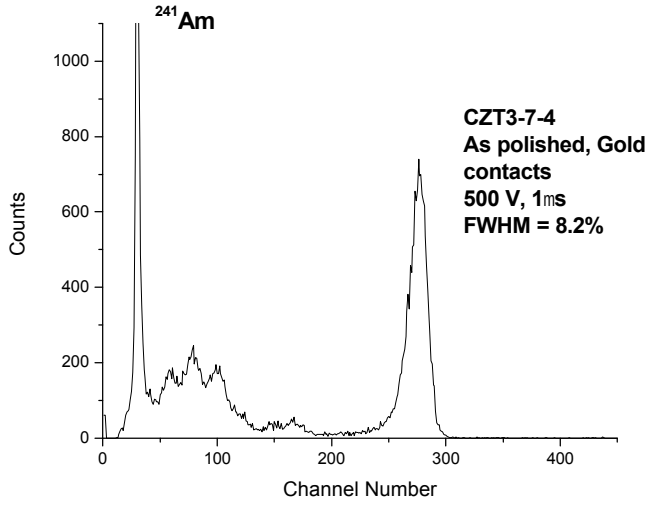

Figure 1. Gamma detector response measurement with ^{241}Am source, 500 V, 1 μs for CZT3-7-4 as polished with Au contacts on the surface. FWHM = 8.2% at ~60 keV.

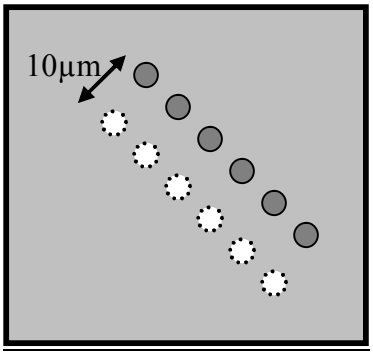

Figure 2. Scheme used for laser treatment of CZT3-7-4 surface by Argon ion laser. The dark fiducial marks were treated with ~20 mW laser power with 10 second (s) exposure time. The lighter regions were treated with the following exposure times and approximate powers: (1) 1.7 mW, 40 s, (2) 850 μW, 40 s, (3) 425 μW, 40 s, (4) 170 μW, 200 s, (5) 425 μW, 200 s, (6) 1.7 mW, 80 s.

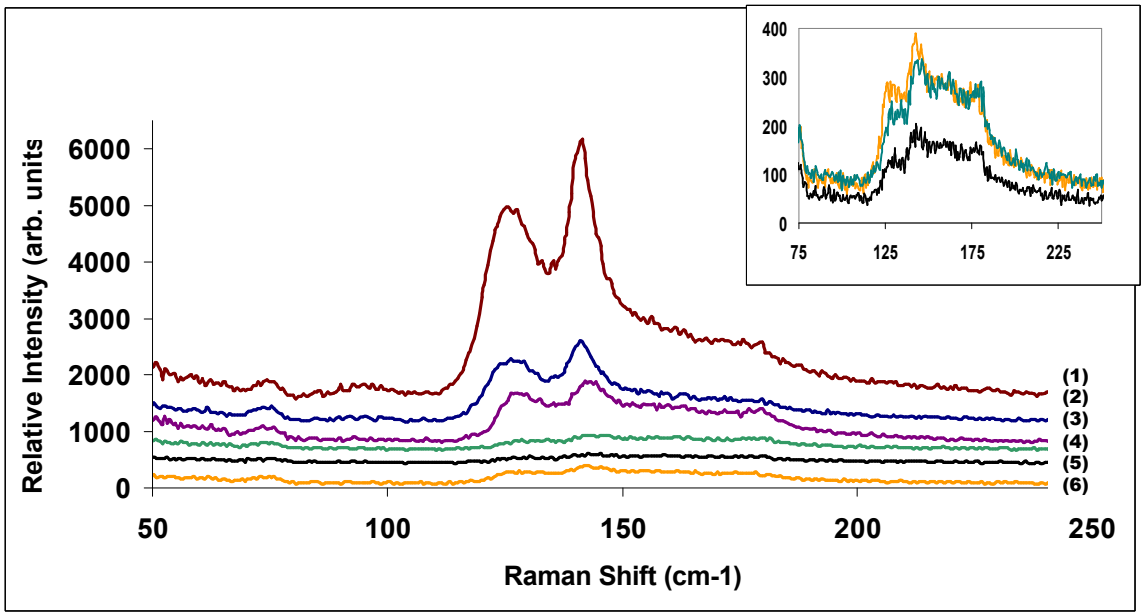

Figure 3: Raman spectra on Cd-terminating face of CZT crystal of varying laser power treatments and are numbered as follows: (1) 1.7 mW, 80 s, (2) 1.7 mW, 40 s, (3) 425 µW, 200 s, (4) 170 µW, 200 s, (5) 425 µW, 40 s, (6) 850 µW, 40 s. Spectra are offset for clarity. Inset shows zoom in of spectra (no offset applied) for spots (4), (5), and (6).

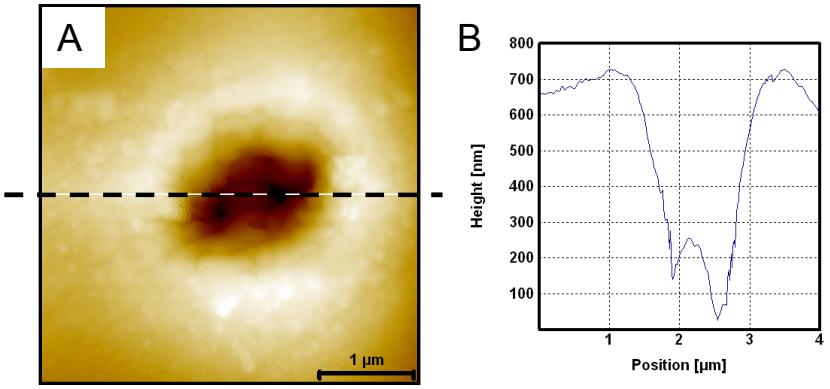

Figure 4. (A) AFM topographic image and (B) corresponding line scan for heavily damaged marker region on Cd-terminating face of CZT3-7-4. Dashed line in (A) indicates location of line profile.

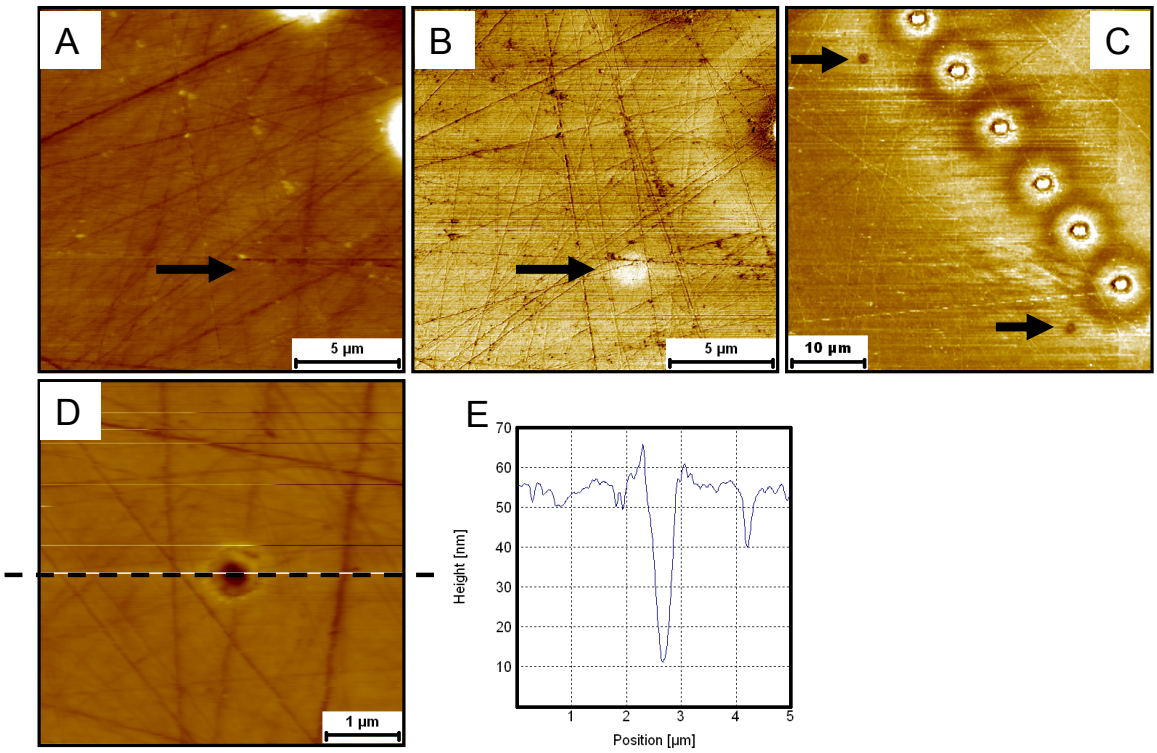

Figure 5. (A) Topographic and (B) lateral force (friction) images of Raman exposed spot (~1.7 mW, 80 s) on Cd terminated side of CZT3-7-4. Arrows indicate location of Raman exposure. Damage to the crystal surface is observed in lateral image, but no damage is observed in topography. Lateral force image of the Te terminated side of CZT3-7-4 (C) shows damage to the crystal in two spots (both ~1.7 mW laser power, indicated by black arrows). The topographic image (D) and corresponding line profile (E) of the topmost spot reveal more obvious surface damage due to laser exposure. Collectively, these images show damage to the crystal surface caused by the Raman laser.

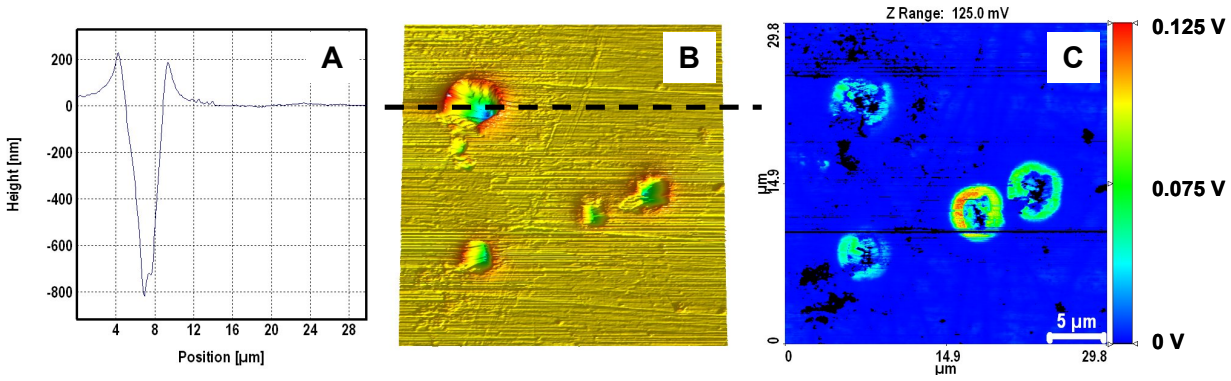

Figure 6. (A) Line profile, (B) 3-D topographic AFM image, and (C) corresponding C-AFM image of Raman laser induced damage on CZT3-7-8. The dashed line in the topographic image indicates location of line profile and shows that the depth of the localized Raman damage is ~800 nm. Surface topography and conductivity map were recorded simultaneously with +7 V bias on the CZT crystal. C-AFM image shows that areas of Raman exposure are more conductive than surrounding CZT crystal surface.

References:

1. T. E. Schlesinger, J. E. Toney, H. Yoon, E. Y. Lee, B. A. Burnett, L. Franks, and R. B. James, *Mater. Sci. Eng. R* 32, 103-189 (2001).
2. J. F. Butler, C. Lingren, and F. P. Doty, *IEEE Trans. Nucl. Sci* 6, 605 (1992).
3. A. E. Bolotnikov, G. S. Camarda, G. A. Carini, Y. Cui, L. Li, and R. B. James, *Nucl. Instrum. Methods A* 571, 687-698 (2007).
4. A. Burger, K. Chattopadhyay, H. Chen, X. Ma, J. O. Ndap, M. Schieber, T. E. Schlesinger, H. W. Yao, J. Erickson, and R. B. James, *Nucl. Instrum. Methods A* 448, 586-590 (2000).
5. G. A. Carini, A. E. Bolotnikov, G. S. Camarda, G. W. Wright, R. B. James, and L. Li, *Appl. Phys. Lett.* 88, 143515 (2006).
6. M. C. Duff, D. B. Hunter, A. Burger, M. Groza, V. Buliga, and D. R. Black, *App. Surf. Sci.* 254, 2889-2892 (2008).
7. T. Wang, W. Q. Jie, and D. M. Zeng, *Mater. Sci. Eng. A* 472, 227-230 (2008).
8. J. R. Heffelfinger, D. L. Medlin, and R. B. James, *MRS Symp. Ser.* 487, 33 (1998).
9. M. Schieber, T. E. Schlesinger, R. B. James, H. Hermon, H. Yoon, and M. Goorsky, *J. Cryst. Growth* 237-239, 2082 (2002).
10. J. Shen, D. K. Aidun, L. Regel, and W. R. Wilcox, *J. Cryst. Growth* 132, 250 (1993).
11. C. Szeles, and M. C. Driver, *SPIE* 3446, 1 (1998).

12. A. E. Bolotnikov, G. S. Camarda, G. A. Carini, Y. Cui, L. Li, and R. B. James, *Nucl. Instrum. Methods A* 579, 120-124 (2007).
13. B. A. Brunett, J. M. V. Scyoc, N. R. Hilton, J. C. Lund, R. B. James, and T. E. Schlesinger, *IEEE Trans. Nucl. Sci* 46, 237-242 (1999).
14. B. A. Brunett, J. M. V. Scyoc, T. E. Schlesinger, and R. B. James, *Nucl. Instrum. Methods A* 458, 76-84 (2001).
15. M. C. Duff, D. B. Hunter, A. Burger, M. Groza, J. P. Bradley, G. Giles, Z. Dai, D. R. Black, H. Burdette, and A. Lanzirotti, *J. Mater. Res.* in press (2009).
16. S. A. Hawkins, E. V. -Aleman, M. C. Duff, D. B. Hunter, A. Burger, M. Groza, V. Buliga, and D. R. Black, *J. Electron. Mater.* 37, 1438-1443 (2008).
17. G. Koley, J. Liu, and K. C. Mandal, *Appl. Phys. Lett.* 90, 102121 (2007).
18. G. A. Carini, A. E. Bolotnikov, G. S. Camarda, and R. B. James, *Nucl. Instrum. Methods A* 579, 120-124 (2007).
19. M. C. Duff, D. B. Hunter, P. R. Nuessle, D. R. Black, H. Burdette, J. Woicik, A. Burger, and M. Groza, *J. Electron. Mater.* 36, 1092 (2007).
20. A. Ruzin, I. Torchinski, and I. Goldfarb, *Semicond. Sci. Technol.* 19, 644-647 (2004).
21. H. Huang, J. Xu, J. Wang, C. Zhang, Y. Mo, S. Pan, and G. Zhang, *SPIE Proceedings* 4454, 244 (2001).
22. S. S. Islam, S. Rath, K. P. Jain, S. C. Abbi, C. Julien, and M. Balkanski, *Phys. Rev. B* 46, 4982 (1992).
23. K. Prabakar, S. Venkatachalam, Y. L. Jeyachandran, S. K. Narayandass, and D. Mangalaraj, *Mater. Sci. Eng. B* 107, 99 (2004).
24. M. G. Sridharan, M. Mekaladevi, S. K. Narayandass, D. Mangalaraj, and H. Chul Lee, *J. Optoelectron. Adv. Mater.* 7, 1479 (2005).
25. M. G. Sridharan, S. K. Narayandass, and H. Chul Lee, *J. Optoelectron. Adv. Mater.* 7, 1483 (2005).
26. M. G. Sridharan, S. K. Narayandass, D. Mangalaraj, and H. Chul Lee, *Vacuum* 70, 511 (2003).
27. L. Li, F. Lu, C. Lee, G. W. Wright, D. R. Rhiger, S. Sen, K. S. Shah, M. R. Squillante, L. Cirinano, R. B. James, A. Burger, P. Luke, and R. Olson, *SPIE* 4784, 76 (2003).
28. A. S. Pine, and G. Dresselhaus, *Phys. Rev. B* 4, 356 (1971).
29. H. R. Vydyanath, J. Ellsworth, J. J. Kennedy, B. Dean, C. J. Johnson, G. T. Neugebauer, J. Sepich, and P.-K. Liao, *J. Vac. Sci. Technol. B* 10, 1476 (1992).